Comparison of different tyre models for tyre/road noise applications

Ladan Pahlevani, Denis Duhamel, Gwendal Cumunel, Yin Hai-Ping

Comparison of different tire models for tire/road noise applications

Pahlevani Ladan

Université Paris-Est, Laboratoire Navier, ENPC-IFSTTAR-CNRS, UMR 8205, Ecole des Ponts ParisTech, 6-8 avenue Blaise Pascal, 77455 Marne la Vallée, France
E-mail: ladan.pahlevani@enpc.fr

Duhamel Denis

Université Paris-Est, Laboratoire Navier, ENPC-IFSTTAR-CNRS, UMR 8205, Ecole des Ponts ParisTech, 6-8 avenue Blaise Pascal, 77455 Marne la Vallée, France
E-mail: denis.duhamel@enpc.fr

Cumunel Gwendal

Université Paris-Est, Laboratoire Navier, ENPC-IFSTTAR-CNRS, UMR 8205, Ecole des Ponts ParisTech, 6-8 avenue Blaise Pascal, 77455 Marne la Vallée, France
E-mail: gwendal.cumunel@enpc.fr

Yin Hai-Ping

Université Paris-Est, Laboratoire Navier, ENPC-IFSTTAR-CNRS, UMR 8205, Ecole des Ponts ParisTech, 6-8 avenue Blaise Pascal, 77455 Marne la Vallée, France
E-mail: honore.yin@enpc.fr

Abstract: In terms of safety and environment, the reduction of noise generated by tire vibrations on roads has a significant importance. In order to study the vibration properties of a tire, various models have been presented in the literature. The main purpose of the current study is a brief review of the characteristics of some models. It is supposed that the tire is subjected to an excitation caused by the contact between the tire and the road. Subsequently, the dynamic behaviour of these models are studied and compared with each other. The effects of inflation pressure and the tread patterns on the dynamic behaviour of the mentioned models are examined. For verification, the dynamical behaviour of the tire is studied experimentally. Application of the present study can be contemplated in the prediction of rolling noise and rolling resistance.

Keywords: Tire; Noise; Vibration; Modelling; Circular ring; Beam; Orthotropic plate; Rotation; Inflation pressure; Periodic structure; Finite element; Experimental result.

1 Introduction

Noise and vibrations are important problems in vehicles, see Qatu et al (2009); Qatu (2012) for reviews on these subjects. In this field, noise coming from tyres is especially important. So a lot of researches have been done on tyre noise generation during the last decades, see for instance Kropp (1999) for an explanation of the different mechanisms of noise generation and for an example of global modelling. The vibrations of tires are an important mechanism leading to noise generation. So different models have been proposed in the past to describe the vibration properties of vehicle tires. In this purpose, one of the simplest methods is the model of a rotating ring on an elastic foundation. Due to its completeness and simplicity, since the 1960s, this method has drawn the attractions of numerous researchers. The development of the method was pioneered by Clark (1965), Tielking (1965), and Bohm (1966) who presented a method for calculating the dynamic behaviour of a loaded pneumatic tire modelled as an elastically supported cylindrical shell. In these works, the tire sidewall effects were modelled by the radial springs. Pacejka (1971) modelled the tire as a circular ring under pressure. By considering the circumferential springs for the elastic foundation, he developed models for the lateral vibration. The effect of structural damping on the study of the dynamic response of the classical ring on the foundation was considered for the first time by Padovan (1976). Later, Potts et al. (1977) studied the vibration of a rotating ring on an elastic foundation in terms of the material and geometric properties of the tire. In order to study the free vibration of a circular ring tire located on an elastic foundation, a finite element method was presented by Kung (1987). Huang and Soedel (1987a,b) and Huang (1992) studied the response of a rotating ring subjected to harmonic and periodic loadings. In Wei et al. (2008), the authors proposed an analytical approach to analyse the forced transient response of tires modelled as a ring on an elastic foundation. The next method to model the tire structure is the model of a Timoshenko beam. Pinnington and Briscoe (2002) modelled the tire belt based on the tensioned Timoshenko beam in order to derive arbitrary sidewall impedances. They developed a one-dimensional wave model to describe the tire dynamics. The waves, which propagate along the tire, take shear and rotational effects into account. Recently, Vu et al. (2017) presented a circular beam model based on the timoshenko beam theory to study the dynamic behaviour of the tire around its linear/nonlinear state. The validity of the circular ring models is limited to frequencies less than 400Hz, when the wavelength is large enough compared to the width of the tire.

In order to study the vibrational tire properties for higher frequencies, Kropp (1989), proposed the orthotropic plate model on a winkler foundation, where the tire belt is modelled as a finite plate which has different tangential and lateral properties. The foundation represents the effect of sidewalls as well as the inflation pressure. Also, the external tension forces due to the inflation pressure are considered in this model. In Hamet (2001); Muggleton et al (2003), the authors proposed an analytical approach to study the frequency or impulse responses of a tire modelled by one or two thin orthotropic plate under tension supported by an elastic foundation. Later, Larsson and Kropp (2002) developed a double-layer tire model including the tangential motion and the local deformation of the tread. Their model is appropriate for the modelling of radial and tangential vibrations in the high-frequency range

and was compared to the circular ring model in Perisse and Hamet (2000a). However, the model of the orthotropic plate is completely dependent on the results of experiments. In order to estimate the structural properties of the orthotropic plate tire model, Perisse et al. (2000b); Perisse (2002) presented a procedure for the experimental modal testing of a smooth tire for low and medium frequencies. The case of circular rotating shells was described by Kim and Bolton (2001, 2004) who mainly solved the analytical shell equations to estimate the influence of rotation. Another curved plate model was developped by Pinnington (2006a,b) It allows to take into account the effects of curvature, shear stiffness, rotary inertia, tension, rotational speed and air pressure.

However, applying finite element (FE) approaches, one can model more accurately the structural features of a tire. Thus, especially during the past decade, a considerable number of studies have been focused to investigate the wave propagation in a model of a tire based on FE techniques. Narasimha Rao and Kumar (2007) used dynamic finite element models of tyres for simulating braking and corning. Richards (1991) considered finite elements for low frequency cases but has included the air cavity. Lopez et al (2007, 2009) have computed tire vibrations by the FE approach using a modal superposition around deformed tyres and have included rotational effects. Their computations were limited to 500Hz. Brinkmeier et al (2008, 2007) used the FE with an ALE approach to compute tyre vibrations up to 850Hz. A similar FE model including nonlinearities was developed by Zhang et al (2004) for the modal analysis of truck tyres.

Another possibility is to consider the tyre as a periodic structure. Brillouin (1953) and Mead (1996) applied the Floquet's principle or the transfer matrix to study the wave propagation in a three-dimensional (3D) periodic structure. In Houillon et al. (2005) and Mace et al. (2005), the authors developed a FE method to determine the propagation constants and wave modes. Their works were focused on obtaining dispersion relations and their application in energetic methods. Recently, Duhamel et al. (2006) employed a similar method to calculate dispersion relations but for point force responses. Their approach was called the Waveguide Finite Element (WFE). Furthermore, this technique was applied by Waki et al. (2009) to predict the free wave propagation and the forced response of a tire. The results obtained by using WFE methods is similar to those obtained with the classical FE approach. But, the computational cost of the WFE method is very low compared to the usual FE. To this end, one can easily use this model to analyse structures with complex geometries and material distributions. In addition, applying a reduction technique, the number of degrees of freedom (DOF) in a periodic element can be greatly reduced so that it can significantly shorten the computation time.

In the current work, we mainly review the above mentioned models of tire with a focus on their vibrational response. For this purpose, we calculate the dynamic behaviour of these models, discuss their assumptions and limitations, and compare their results with the experimental results. In case studies, the effect of inflation pressure in the tire is studied. In order to verify the results given by the periodic 3D model, a full 3D tire model is analysed numerically via a FE technique.

This paper is organized as follows. In the next section, a brief review of the characteristics of tire models will be addressed. Section 3 devotes to estimate the structural and material properties required in circular ring and orthotropic models. Some numerical results are reported and discussed in section 4. Finally, section 5 includes concluding remarks.

Figure 1 Single Degree of Freedom System

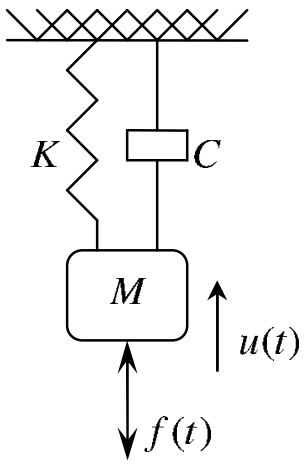

2 Brief review on tire models

In this section, we summarize the existing models of tire proposed in the literature and discuss the assumptions, limitations, and drawbacks of each model. The models can be classified into seven categories; a simple model based on a single degree of freedom (SDOF) system, rotating ring model, Timoshenko circular beam model, orthotropic plate model, periodic 3D model, full 3D model, and experimental model.

The properties of the above mentioned models are demonstrated in detail in the following.

2.1 Single Degree of Freedom (SDOF) System

Figure 1 shows the basic model for the SDOF system. This model consists of a concentrated mass, M, attached to a spring with stiffness K and a viscous dashpot, C. $F(t)$ and $u(t)$ are general time-varying force and displacement responses. Considering an excitation of the form $f(t) = fe^{i\omega t}$, and a solution of the form of $u(t) = ue^{i\omega t}$, the equation of motion can be rewritten as (see Ewins (1986))

$$(-\omega^2 M + i\omega C + K)ue^{i\omega t} = fe^{i\omega t}. \tag{1}$$

Therefore, the receptance frequency response function is

$$G(\omega) = \frac{1}{(-\omega^2 M + i\omega C + K)}. \tag{2}$$

As it is observed, mathematically, this model is very simple. For the tire model, M represents the mass of the tire and the stiffness and inflation in the tire are considered by K. As expected, the results obtained by this model are not as accurate as for the other models. The SDOF model of tire can be utilized in fundamental studies or for dynamics at very low frequencies. It can not really be used for noise predictions.

2.2 Rotating Ring Model

The rotating ring model is one of the simplest methods used to model a tire. In this model, it is supposed that the car tire is composed of two main parts; the belt band (tread) and the sidewalls. Based on the inflation pressure of the tire, the sidewall moves along three directions: radial, tangential, and lateral. Here, the tread is modelled as a rotating ring and the elastic properties of sidewalls are modelled by the distributed springs, k_r and k_θ in radial and circumferential directions, respectively, i.e. the lateral stiffness is ignored (Figure 2). It is assumed that there is a punctual contact between the ring and the road (refer to Huang and Soedel (1987b), distributed loads over the contact area can be approximated by a point load). In addition, the slip between the ring and the road surface is ignored. Considering u_r and u_θ as the displacements in the radial and tangential directions, respectively, for the rotating tire with no contact, the equations of motion are written as (see Huang and Soedel (1987b))

$$\begin{aligned}
&\frac{EI}{R^4}(u_r^{''''} - u_\theta^{'''}) + \frac{EA}{R^2}(u_r + u_\theta^{'}) + \frac{pb}{R}(u_r + 2u_\theta^{'} - u_r^{''}) \\
&\qquad +k_r u_r + \rho A\Omega^2(2u'_\theta - u''_r), +\rho A(\ddot{u}_r - 2\Omega\dot{u}_\theta) = q_r \\
&\frac{EI}{R^4}(u'''_r - u''_\theta) - \frac{EA}{R^2}(u'_r + u''_\theta) + \frac{pb}{R}(u_\theta - 2u'_r - u''_\theta) \\
&\qquad +k_\theta u_\theta - \rho A\Omega^2(2u'_r + u''_\theta) + \rho A(\ddot{u}_\theta + 2\Omega\dot{u}_r) = q_\theta,
\end{aligned} \tag{3}$$

where, R, b, h, and ρ are the mean radius, tread width, averaged thickness, and density of the tire, respectively. EI and EA indicate the bending and the membrane stiffness, respectively. I and A are the moment inertia and surface of the ring cross-section and E corresponds to the Young's modulus of the tire. p denotes the internal pressure and Ω indicates the rotational velocity. $q(q_r, q_\theta)$ applies the external load of the system. In these equations, primes and dots indicate the differentiations with respect to theta and t, respectively. By applying a modal analysis, for each mode the displacements, u_r and u_θ, can be obtained as following (see Huang and Soedel (1987b))

$$(u_r, u_\theta) = \sum_{n=-\infty}^{n=+\infty} (A_n, B_n) e^{i(n\theta + \omega_n t)}, \tag{4}$$

where, ω_n indicates the natural frequency of the system and A_n and B_n are constants. During the rotation, the circular ring is subjected to the two external loadings; the first one is corresponding to the weight of the vehicle and the other is the excitation due to the contact between the ring and the road. In the current study, the weight of the vehicle is ignored. Generally, the equation of motion in the time domain can be expressed as

$$M\ddot{u}(t) + C\dot{u}(t) + Ku(t) = q(t), \tag{5}$$

where M, C, and K are the mass, damping and stiffness matrices, respectively, while u and q denote the displacement and force vectors. In the frequency domain, we have

$$u(\omega) = G(\omega)q(\omega), \tag{6}$$

where G is the Green's function which can be approximated by a linear combination of N modes as

$$G(\omega) = [-\omega^2 M + i\omega C + K]^{-1} = \sum_{n=1}^{N} \frac{\varphi_n \varphi_n^t}{(-\omega^2 + 2i\xi_n \omega_n \omega + \omega_n^2)}, \tag{7}$$

where ξ_n and φ_n indicate the damping and the mass-normalized mode shape for mode n, respectively. In order to calculate the natural frequencies of the system, we can substitute Eq. 4 into Eq. 3 and considering the harmonic function $e^{in\theta}$ so,

$$k_n \begin{bmatrix} A_n \\ B_n \end{bmatrix} = \begin{bmatrix} 0 \\ 0 \end{bmatrix}, \tag{8}$$

where,

$$\begin{aligned}
k_n &= \begin{bmatrix} -i(d_1 - 2\Omega\omega_n) & d_2 - \omega_n^2 \\ d_3 - \omega_n^2 & i(d_1 - 2\Omega\omega_n) \end{bmatrix}, \\
d_1 &= \frac{1}{\rho A}[n^3 \frac{EI}{R^4} + n\frac{EA}{R^2} + 2n\frac{pb}{R} + 2n\rho A\Omega^2], \\
d_2 &= \frac{1}{\rho A}[n^2 \frac{EI}{R^4} + \frac{EA}{R^2} + \frac{pb(n^2+1)}{R} + \rho A n^2\Omega^2 + k_\theta], \\
d_3 &= \frac{1}{\rho A}[n^4 \frac{EI}{R^4} + \frac{EA}{R^2} + \frac{pb(n^2+1)}{R} + \rho A n^2\Omega^2 + k_r].
\end{aligned} \tag{9}$$

If the determinant of k_n equals zero, the natural frequencies of the system are easily computed as the roots of this equation

$$\omega_n^4 - (4\Omega^2 + d_2 + d_3)\omega_n^2 + 4d_1\Omega\omega_n + d_2 d_3 - d_1^2 = 0. \tag{10}$$

This model is interesting for low frequencies computations. It has some limitations as it cannot take into account the non linear quasi-static deformation created by the contact with the road but only the effect of pre-stress coming from the internal pressure. It allows to consider the effect of rotation of the tire. Moreover this model makes the assumption that the displacement is uniform along the width of the tire so that a beam model can be used.

2.3 Timoshenko Circular Beam Model

In the Timoshenko circular beam model, the belt is modelled as a Timoshenko beam to accommodate bending, shear, and the rotary inertia effects that are significant at high frequencies. Similar to the circular ring model presented in the previous section, the sidewall of the tire is replaced by the radial and tangential springs, k_r and k_θ. Considering R as the mean radius of the tire, in the linear case, one can obtain the equations of motion of the Timoshenko circular beam as under the form of (see Vu et al. (2017))

$$\begin{aligned}
&(\frac{GA}{R} + \frac{GI}{R^3})(\frac{u_r^{''} - u_\theta^{'}}{R} + \alpha^{'}) - \frac{EA}{R}(\frac{u_r + u_\theta^{'}}{R}) - \frac{EI}{R^3}(\frac{u_r + u_\theta^{'}}{R} - \alpha^{'}) + p - k_r u_r \\
&-\rho A\Omega^2(-R + u_r^{''} - 2u_\theta^{'} - u_r) + q_r = \rho A\ddot{u}_r + 2\rho\Omega A(\dot{u}_r^{'} - \dot{u}_\theta),
\end{aligned}$$

Figure 2 Circular ring model

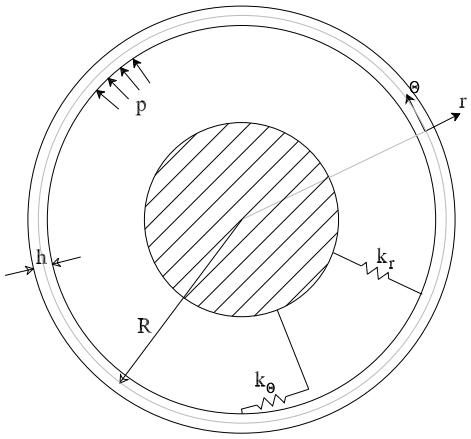

$$\begin{aligned}
&\frac{EA}{R}(\frac{u_r^{'}+u_\theta^{''}}{R})+\frac{EI}{R^3}(\frac{u_r^{'}+u_\theta^{''}}{R}-\alpha^{'})+(\frac{GA}{R}+\frac{GI}{R^3})(\frac{u_r^{'}-u_\theta}{R}+\alpha)\\
&-k_\theta u_\theta-\rho A\Omega^2(u_\theta^{''}+2u_r^{'}-u_\theta)+q_\theta=\rho A\ddot{u}_\theta+2\rho\Omega A(\dot{u}_r+\dot{u}_\theta^{'}),\\
&\frac{EI}{R^2}(-\frac{u_r^{'}+u_\theta^{''}}{R}+\alpha^{''})-(GA+\frac{GI}{R})(\frac{u_r^{'}-u_\theta}{R}+\alpha)-\rho I\Omega^2\alpha^{''}=\rho I\ddot{\alpha}+2\rho\Omega I\dot{\alpha}^{'}.
\end{aligned} \tag{11}$$

where, G and ν indicate the shear modulus and Poisson's coefficient, respectively, and α denotes the rotation along the z axis. The general form of the equation of motion in the time domain is referred by Eq. 5. For the current model, in order to obtain the K matrix, a numerical approach based on the finite difference approximation technique is applied. The finite difference operators are defined as

$$\begin{aligned}
u^{'}(\theta_i)&=\frac{u(\theta_{i+1})-u(\theta_{i-1})}{2h},\\
u^{''}(\theta_i)&=\frac{u(\theta_{i+1})-2u(\theta_i)+u(\theta_{i-1})}{h^2},
\end{aligned} \tag{12}$$

where, $\theta=(\theta_1=0,\theta_2,\ldots,\theta_N=\frac{2\pi(N-1)}{N})$, N is the number of points considered on the circular beam. Note that $u(0)=u(2\pi)$. After calculating the K matrix, we can determine the frequency response function of the system by applying the modal analysis.

Compared with the circular ring model, the Timoshenko beam model allows a better approach of beam deformation. Vu et al. (2017) have also shown that a non linear Timoshenko beam model can take into account the non linear deformation created by a contact with a soft road. Then linear vibrations can be computed as small dynamic perturbations around this quasi-static non linear deformation.

2.4 Orthotropic Plate Model

In this model, the tire is simulated by a three dimensional plate as the tire belt, which has different tangential and lateral properties, and the sidewalls modelled by a thin plate under tension on an elastic foundation (due to the inflation in the tire), see Figure 3. Based on the Kirchhoff hypothesis for thin plates, the equation of motion can be written as (see Kropp (1989))

$$[-T_{0x}\frac{\partial^2}{\partial x^2} - T_{0y}\frac{\partial^2}{\partial y^2} + B_x\frac{\partial^4}{\partial x^4} + 2\sqrt{B_{xy}}\frac{\partial^2}{\partial x^2}\frac{\partial^2}{\partial y^2} + B_y\frac{\partial^4}{\partial y^4} + s + m\frac{\partial^2}{\partial t^2}]u(x,y,t) = F(x,y,t), \quad (13)$$

where T_{0x} and T_{0y} are membrane tensions caused by the air inflation in the tire. B_x, B_y, and B_{xy} are the longitudinal bending, transversal bending, and the cross stiffness of the belt, respectively. For the orthotropic plates $B_{xy} \approx B_x B_y$. s indicates the stiffness of the elastic support of the belt. m and F are the mass of the plate and the acting force per unit area, respectively. In the analysis, only harmonic motions are considered and the common factor $e^{i\omega t}$ is omitted. Material losses are introduced by adding an imaginary part to the bending stiffness, tensions and the stiffness of the foundation. Note that only the radial motion of the tire (the vertical motion of the plate) is considered. The corresponding boundary conditions are defined as $u(x + l_x, y, t) = u(x, y, t)$, i.e. the belt is circular, $u(x, y, t) = 0$ at $y = 0$, $y = l_y$, i.e. the plate is simply supported at the sides, and, $\frac{\partial^2}{\partial y^2}(x, y, t) = 0$ at $y = 0, y = l_y$.

Using the Green's function technique, the solution of the equation can be expressed as following

$$u(x,y,t) = \int\int\int F(x_0,y_0,\tau)G(x,y,t)dx_0dy_0d\tau, \quad (14)$$

where $G(x, y, t)$ is solution of

$$[-T_{0x}\frac{\partial^2}{\partial x^2} - T_{0y}\frac{\partial^2}{\partial y^2} + B_x\frac{\partial^4}{\partial x^4} + 2\sqrt{B_{xy}}\frac{\partial^2}{\partial x^2}\frac{\partial^2}{\partial y^2} + B_y\frac{\partial^4}{\partial y^4} + s + m\frac{\partial^2}{\partial t^2}] \times G(x-x_0,y-y_0,t-\tau) = \delta(x-x_0)\delta(y-y_0)\delta(t-\tau). \quad (15)$$

Modelling the circular tire by an infinitely long strip and calculating the corresponding Green's function in terms of the superposition of normal modes, one can obtain (see Hamet (2001))

$$G(x,y,t) = \frac{4}{l_x l_y}\frac{1}{m}\sum_{n=1}^{\infty} sin(k_{yn}y_0)sin(k_{yn}y) \sum_{m=0}^{\infty}\epsilon_m \frac{cos[k_{xm}(x-x_0)]sin[\Omega_{nm}(t-\tau)]}{\Omega_{nm}} e^{-\eta_{nm}\Omega_{nm}(t-\tau)}H(t-\tau), \quad (16)$$

Figure 3 Orthotropic plate model

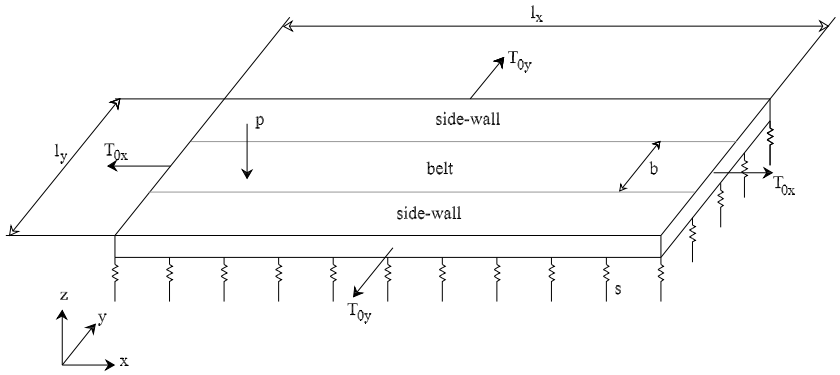

where Ω_{nm} are the eigenfrequencies associated to the wavenumbers $k_{xm} = \frac{2\pi m}{l_x}$ and $k_{yn} = \frac{\pi n}{l_y}$. Ω_{nm} is defined as

$$\Omega_{nm} = Re(\sqrt{[k_{xm}^4 B_x + 2k_{xm}^2 k_{yn}^2 \sqrt{B_x B_y} + k_{yn}^4 B_y + (k_{xm}^2 + k_{yn}^2)T_0 + s]/m}), \tag{17}$$

The constant ϵ has the values $\epsilon_0 = \frac{1}{2}$ and $\epsilon_{m\neq 0} = 1$. η is the damping for each mode which is calculated as

$$\eta = \frac{1}{\Omega_{nm}} Im(\sqrt{[k_{xm}^4 B_x + 2k_{xm}^2 k_{yn}^2 \sqrt{B_x B_y} + k_{yn}^4 B_y + (k_{xm}^2 + k_{yn}^2)T_0 + s]/m}). \tag{18}$$

Compared with the circular ring model, the main advantage of these plate models is to describe non uniform motions along the width of the tire.

2.5 Periodic 3D Model

A symmetrical periodic element of the tire, as shown in Figure 4, is considered. The equation for time harmonic motions of a periodic section can be written as

$$Du = q, \tag{19}$$

where $D = K + i\omega C - \omega^2 M$, is the dynamic stiffness matrix, u and q denote nodal DoFs and the force vector, respectively. K, C, and M are the stiffness, viscous damping and mass matrices which are obtained from conventional FE methods. If D is decomposed into its left (L) and right (R) boundaries, its interior degrees of freedom are indicated by I, and also it is assumed that there are no external forces on the interior nodes, the equation of motion can be expressed as

$$\begin{bmatrix} D_{LL} & D_{LR} & D_{LI} \\ D_{RL} & D_{RR} & D_{RI} \\ D_{IL} & D_{IR} & D_{II} \end{bmatrix} \times \begin{bmatrix} u_L \\ u_R \\ u_I \end{bmatrix} = \begin{bmatrix} q_L \\ q_R \\ 0 \end{bmatrix}. \tag{20}$$

By eliminating the interior degrees of freedom this equation can be condensed, also in order to decrease the number of degrees of freedom, a reduced basis can be used (see Duhamel et al. (2006)). After calculation of wave modes in the system, the frequency response function can be obtained.

This model should lead to exactly the same results as a full finite element computation if the deformation is linear and if the geometry of the tire is periodic along the circumference. With these two assumptions one can get results in a much lower computing time than if a full 3D model was used.

2.6 Full 3D Model

Figure 5 displays a full three-dimensional model of tire considered in this study. This model is devoted solely to the verification of the results obtained by the periodic 3D model. For this purpose, the tire is analysed numerically by the finite element techniques. Abaqus software is applied to model and analyse the tire.

This is the more general approach which could allow to consider non linear behaviors in term of material and geometrical deformations. Complicated geometrical details of the tire could also be described. However, this leads to very heavy computations so that only low frequencies can be computed.

2.7 Experimental study

Finally, the vibrations of the tire are studied experimentally. The type of tire used in this experiment is a Michelin 165/70R13. The inflation pressure of the tire is about 2 bars. Figure 6 shows a schematic of the experiment setup. As it is seen, a freely suspended tire mounted on a steel rim is taken into account. To apply random excitation forces to the tire, an electrodynamic shaker (B&K 4809) is considered. Point mobility is measured with an impedance head (B&K 8001). In this study, only the radial vibration of the tire is measured. Using a Fast Fourier Transformation (FFT) based spectrum analyser, one can obtain the mobility response of the system.

3 Prediction of structural and material properties required in the circular ring and orthotropic models

As described in the previous sections, in order to study the dynamic behaviour of tires, two models of circular ring and orthotropic plate, beside of the SDOF and 3D models, are

Figure 4 Symmetrical periodic element of a tire

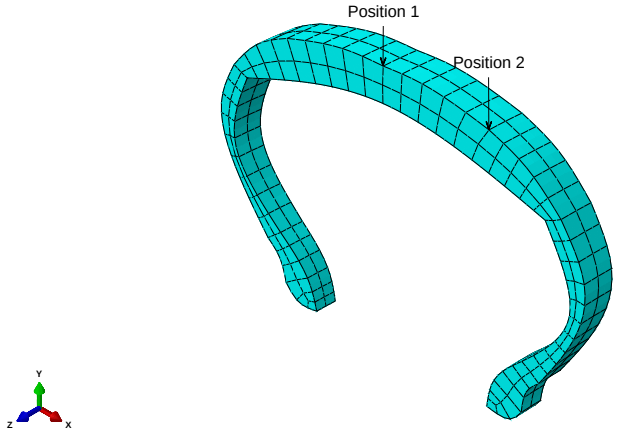

a)

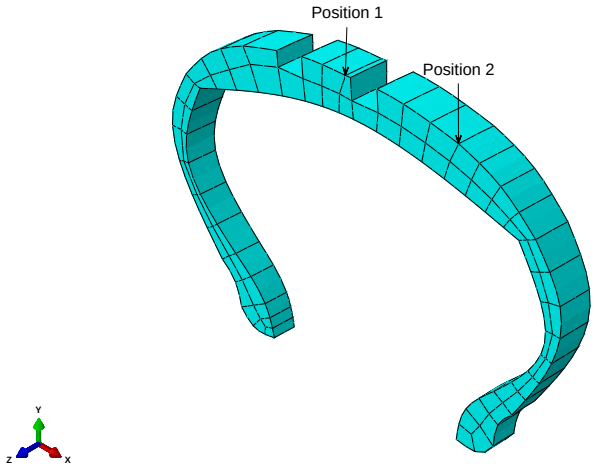

b)

Figure 5 Full 3D model

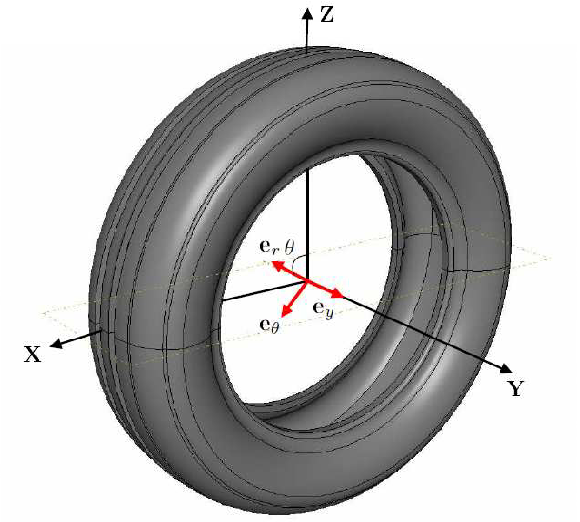

Figure 6 Schematic of the experiment setup

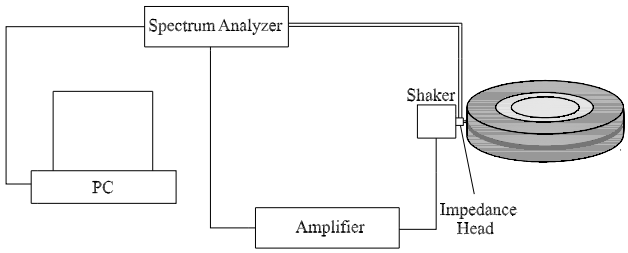

employed. In order to apply these models, first, we require to estimate structural and material data associated to the nature of these models. For this purpose, two studies are conducted; at the first study a homogeneous smooth tire, and at the second one a homogeneous grooved tire are modelled by Abaqus software. For both studies, we consider that the inflation pressure in the tire equals 2 bars. The models have the same cross-sections as in Figures 4(a),(b) but with the full circumference modelled by finite elements. The mechanical and structural properties of the tire are given in Table 1. In the present study, a proportional damping is considered, so that the viscous damping matrix C is defined as

$$C = \alpha M + \beta K, \tag{21}$$

where, M and K are the mass and stiffness matrices of the model respectively. α and β are damping factors whose values are computed based on an experimental measurement on the Michelin R13/165/65 tire in which, $\alpha = 14.4$ and $\beta = 8 \times 10^{-5}$. The radial driving point mobilities corresponding to the smooth and the grooved tires are plotted in Figure 7 for a point force at position 1 in Figure 4 and a receiver at position 2. It can be seen that the response is higher for the grooved tire because the structure has a lower stiffness being made with a reduced thickness at the groove positions.

Internal radius	165.1 mm
Width of tread	165 mm
Height of sidewall	115.5 mm
Young modulus	80 MPa
Poisson coefficient	0.49

Table 1 The mechanical and structural properties of the homogeneous tire

Substituting the first and second resonance frequencies of the given mobility into Eq. 10, one can determine the stiffness of the radial and tangential springs k_r and k_θ as defined in the circular ring model. Table 2 displays the calculated results for both smooth and grooved tires inflated at 2 bars.

Smooth tire	
k_r	$1.244e6\ N/m^2$
k_θ	$9.455e5\ N/m^2$
Grooved tire	
k_r	$1.273e6\ N/m^2$
k_θ	$9.643e5\ N/m^2$

Table 2 Structural and material properties required in the circular ring model of a smooth and grooved tire inflated at 2 bars

In case of the orthotropic plate model, based on the method described by Andersson et al. (2001), the foundation stiffness, s, tensions, T_{0x} and T_{0y}, and bending stiffness, B_x, B_y, and B_{xy}, and their corresponding damping values can be estimated. Detailed formulations to obtain these parameters are given in Appendix A. The results for the considered tires are presented in Table 3.

Figure 7 The radial driving point mobility corresponding to the smooth $(-)$ and grooved tire $(-.-)$ for a force at position 1 and a receiver at position 2.

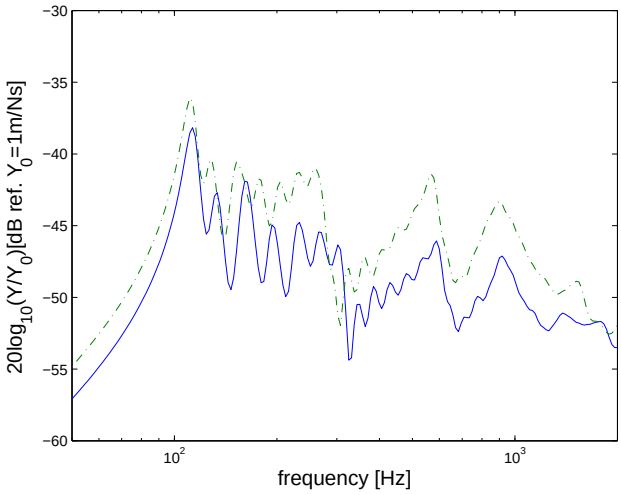

Smooth tire	
T_{0x}	$5e4(1+0.09i)\ N/m$
T_{0y}	$8.5e4(1+0.09i)\ N/m$
B_x	$10.1(1+0.3i)\ Nm$
B_y	$5.1(1+0.3i)\ Nm$
$\sqrt{B_{xy}}$	$7.1(1+0.3i)\ Nm$
s	$3e4(1+0.01i)\ N/m^3$
Grooved tire	
T_{0x}	$4.8e4(1+0.09i)\ N/m$
T_{0y}	$8.3e4(1+0.09i)\ N/m$
B_x	$2.3(1+0.3i)\ Nm$
B_y	$1.2(1+0.3i)\ Nm$
$\sqrt{B_{xy}}$	$1.6(1+0.3i)\ Nm$
s	$3e4(1+0.01i)\ N/m^3$

Table 3 Structural and material properties required in the orthotropic plate model of a smooth and grooved tire inflated at 2 bars

In the next section the vibrational responses obtained by the different methods are studied.

Figure 8 Comparison of the radial driving point mobility obtained by the rotating ring, Timoshenko circular beam, orthotropic plate, and periodic 3D models of tire inflated at 2 bars

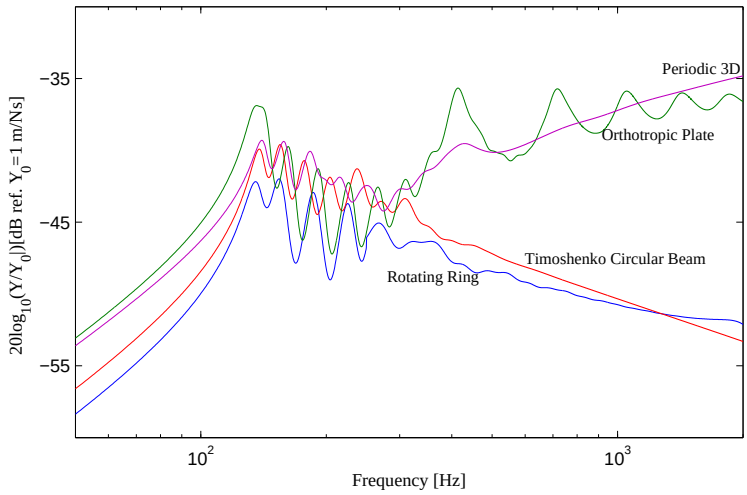

4 Results and discussions

To compare the various models of tire, several numerical studies will be addressed in this section. Furthermore, the effect of inflation pressure as well as of the shape and property of tire are examined. In all the studies presented in this section, the models are subjected to a point force excitation as shown in position 1 of Figure 4, also the reported results are corresponding to the excitation point.

4.1 Homogeneous smooth tire

In the first study, a homogeneous smooth tire inflated at 2 bars is considered. The material properties of the tire are referred in Table 1. The radial point mobility calculated by the models of circular ring, orthotropic plate and periodic 3D are shown in Figure 8.

As it is expected, the models of rotating ring and Timoshenko circular beam are in a good correspondence with the periodic 3D model at low frequencies whereas, at high frequencies, the point mobility given by the orthotropic plate model is very similar to the corresponding results of the periodic 3D model. The circular ring model and the Timoshenko beam model are two beam models with globally the same advantages and defects, so they have similar global behaviours. They provide good results as long as waves do no propagate along the width of the tire which happens around $400Hz$, see Kropp (1989). So above $400Hz$ they can not provide reliable results and they deviate from other more accurate models. The orthotropic plate is close to the finite element model for high frequencies because the response of the tire is rather local in this frequency range and the curvature of the tire or the boundary conditions have little influence here.

The results of a full 3D and a periodic 3D models are compared in Figure 9. It is assumed that the inflation pressure is zero, $p = 0$. Figure 9 demonstrates the point mobilities pertinent

Figure 9 Comparison of the radial driving point mobility obtained by the full (×) and periodic 3D (−) models of tire, the inflation pressure is ignored

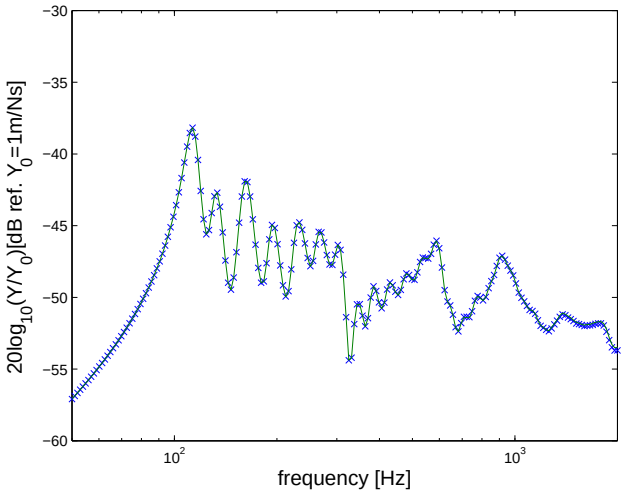

to each model for a point force at position 1 and a receiver at position 2 in Figure 4. As it is seen, the results of two models have a good agreement with each other, whereas, the computation time for the periodic 3D model is significantly less than for the full 3D model. This could be expected as the periodic model is only a numerical tool to accelerate the computation but is based on the same discrete finite element model.

The effect of the inflation pressure is examined in this part. The point mobilities given by the periodic 3D model at pressures 0, 1, and 2 bars are plotted at Figure 10. It is observed that, at low frequencies an increase of the pressure causes the mobilities to decline while the resonance frequencies increase. But, at high frequencies the variation of the inflation pressure has no essential influence on the mobility. The pressure acts by increasing the rigidity of the tire which can be clearly seen at low frequencies where the rigidity dominates. For higher frequencies pre-stress has less influence.

In another study, the variations of k_r and k_θ in the circular ring model with respect to the inflation pressure are displayed in Figure 11. As expected k_r and k_θ increase with the internal pressure as the structure becomes more rigid.

4.2 Homogeneous grooved tire

As it can be seen in Figure 7, when the frequency increases a notable difference between the point mobilities of the smooth tire and the grooved one is observed. To this end, in this part the point mobilities of the homogeneous grooved tire obtained by the different models of tire are studied. We assume that the inflation pressure of the tire is 2 bars. Figure 12 illustrates the results of the different models. Comparison of Figures 8 and 12 shows that, when the tread patterns are considered, the difference of point mobilities between the 3D periodic and the other models increases. Interestingly, this discrepancy is noticeable especially at low frequencies for the circular ring model and high frequencies for the orthotropic model,

Figure 10 The effect of inflation pressure on the radial driving point mobility obtained by the periodic 3D model of tire

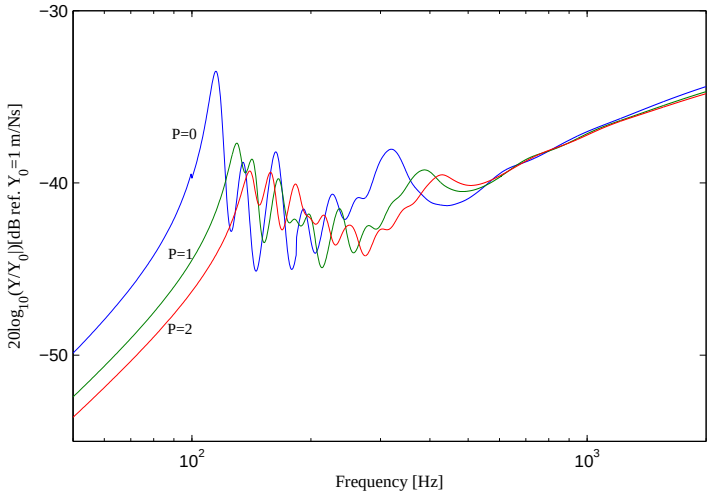

Figure 11 The variations of k_r (continuous line) and k_θ (dashed line) in the circular ring model with respect to the inflation pressure

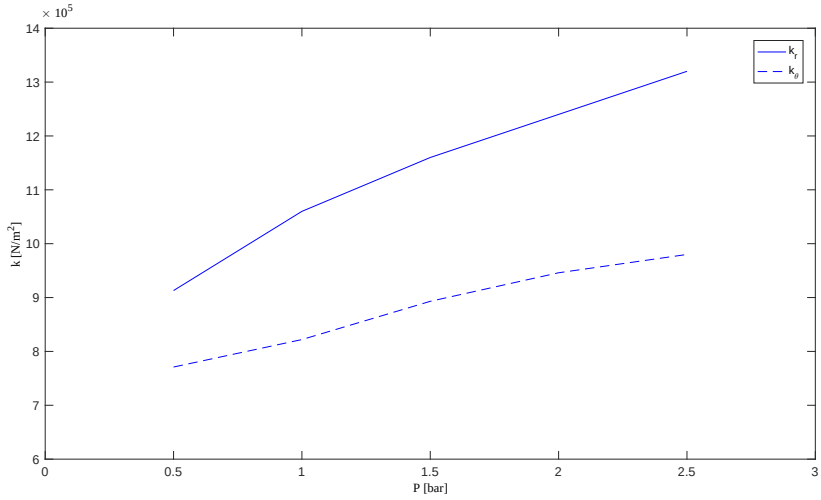

Figure 12 Comparison of the radial driving point mobility obtained by the rotating ring, Timoshenko circular beam, orthotropic plate, periodic 3D, and experimental models of tire inflated at 2 bars

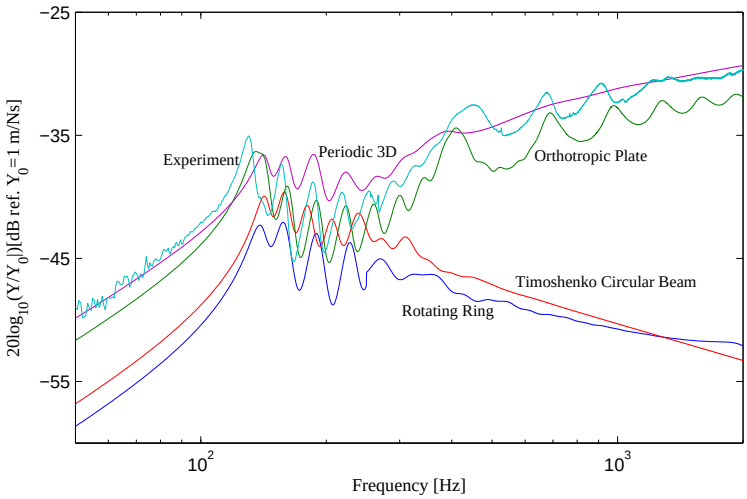

where those models are valid. It can be due to the fact that intrinsically, the circular ring and orthotropic plate models are very simple models of a tire in which the details pertinent to the physical characteristics of a real tire are ignored. On the contrary the periodic finite element model can take into account the geometrical change induced by the groove. One also see that it give results close to the experiment.

4.3 Non-homogeneous grooved tire

Finally, a non-homogeneous grooved tire, modelled by a periodic 3D method is studied (Figure 13). The inflation pressure of the tire is 2 bars. The structural and material properties of the tire are presented in Table 4. Figure 14 illustrates the results corresponding to the radial point mobility of the model. The result is similar to the curve in Figure 12.

5 Conclusion

In summary, we outlined the characteristics of various models of tire as a SDOF system, circular ring, orthotropic plate, 3D, and experimental models. When the tire is subjected to an excitation, we compared the vibrational responses of the models. Generally, the results demonstrated that the circular ring models are valid for low frequencies while the orthotropic plate model provides reasonable result in high frequencies. Also, the point mobility of the tire obtained from 3D and experimental models well agreed with each other. In addition, the effect of the inflation pressure as well as tread patterns were studied. It is observed that there is a significant discrepancy between the calculated point mobility and also the resonance frequency for different pressures at low frequency but by increasing the frequency the discrepancy fades away. Moreover, considering of tread patterns plays an essential role

Figure 13 Cross section of a non-homogeneous grooved tire

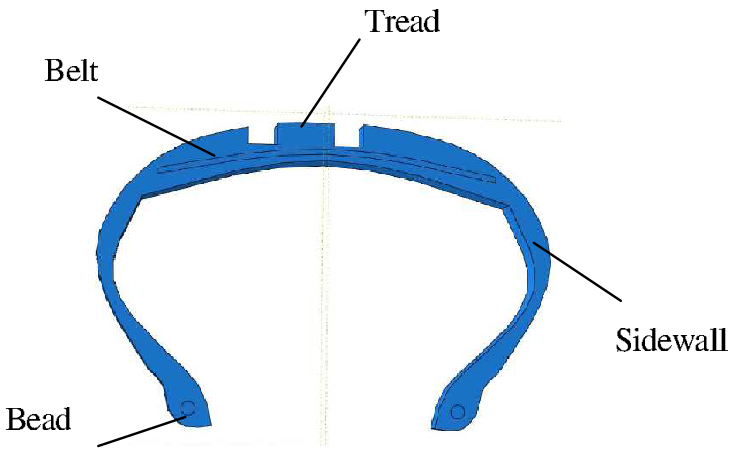

Figure 14 The radial point mobility of a non-homogeneous grooved tire modelled by a periodic 3D approach

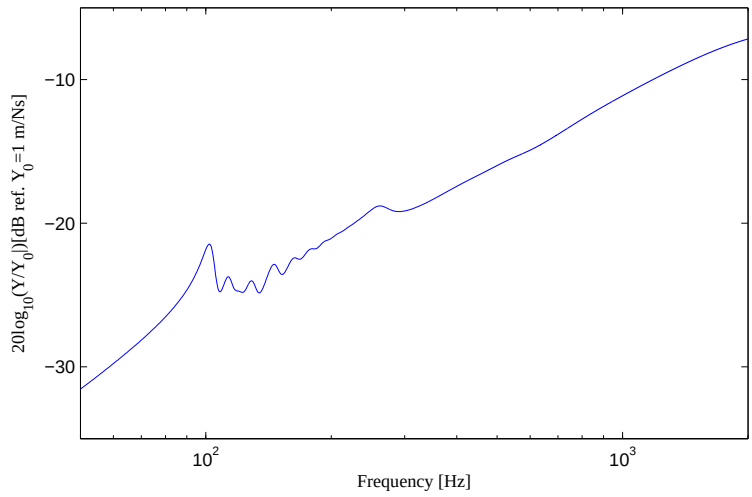

Part	Parameter	Value
Tread	ρ	$1000\ kg/m^3$
	E	$7\ Mpa$
	ν	0.49
Belt	ρ	$2014\ kg/m^3$
	E_x	$660\ Mpa$
	E_y	$9\ Mpa$
	ν_{xy}	0.4
	G_{xy}	$183\ Mpa$
Sidewall	ρ	$1000\ kg/m^3$
	E	$109\ Mpa$
	ν	0.48
Bead core	ρ	$7850\ kg/m^3$
	E	$162.6\ Gpa$
	ν	0.33

Table 4 The mechanical and structural properties of the non-homogeneous tire (see Nguyen (2008))

in the results given by 3D models whereas it has no considerable effect on the results of other numerical models. It can be due to the simple nature of these models. Finally, the point mobility of the tire with a non-homogeneous material was reported in the current work. The presented study may find potential applications in the study of rolling noise and rolling resistance.

References

Andersson, P., Larsson, K. and Kropp, W. (2001) *A method for experimental collection of global material data for tires*, Nordic Vibration Research, Stockholm, Sweden (The Scandianvian Vibration Society, www.svib.se).

Bohm, F. (1966), 'Mechanik des gurtelreifens', *Ingenicar-Archiv* Vol. 35, pp.82-101.

Brillouin, L. (1953) *Wave propagation in periodic structures*, second edition, Dover, New York.

Brinkmeier, M., Nackenhorst, U., Petersen, S. and Von Estorff, O. (2008) 'A finite element approach for the simulation of tire rolling noise', *Journal of Sound and Vibration*, Vol. 309, No 1-2, pp.20-39.

Brinkmeier, M., Nackenhorst, U. and Ziefle, M. (2007) 'Finite element analysis of rolling tires–A state of the art review', *Proceeding of the International CTI Conference Automotive Tire Technology*, pp.1-10, Stuttgart, Germany.

Clark, S.K. (1965) 'The rolling tire under load', *SAE Paper 650493*.

Duhamel, D., Mace, B.R. and Brennan, M.J. (2006) 'Finite element analysis of the vibrations of waveguides and periodic structures', *Journal of Sound and Vibration*, Vol. 294, No. 1-2, pp.205-220.

Ewins, D.J. (1986) *Modal testing: theory and practice*, Research studied press LTD, Letchworth Hertfordshire, England.

Hamet, J.F. (2001) 'Tire/road noise: time domain Green's function for the orthotropic plate model', *Acustica*, Vol. 87, No. 4, pp.470-474.

Houillon, L., Ichchouh, M.N. and Jezequel, L. (2005) 'Wave motion in thin-walled structures', *Journal of Sound and Vibration*, Vol. 281, No. 3-5, pp.483-507.

Huang, S.C. and Soedel, W. (1987) 'Effects of coriolis acceleration on the free and forced in-plane vibrations of rotating rings on elastic foundation', *Journal of Sound and Vibration*, Vol. 115, No. 2, pp.253-274.

Huang, S.C. and Soedel, W. (1987) 'Response of rotating rings to harmonic and periodic loading and comparison with the inverted problem', *Journal of Sound and Vibration*, Vol. 118, No. 2, pp.253-270.

Huang, S.C. (1992) 'The vibration of rolling tires in ground contact', *International Journal of Vehicle Design*, Vol. 13, No. 1, pp.78-95.

Kim, Y.J. and Bolton, J.S. (2001) 'Modeling tire treadband vibration', Inter-noise 2001, The Hague, The Netherlands.

Kim, Y.J. and Bolton, J.S. (2004) 'Effects of rotation on the dynamics of a circular cylindrical shell with application to tire vibration', *Journal of Sound and Vibration*, Vol. 275, No. 3-5, pp.605-621.

Kropp, W. (1989) 'Structure borne sound on a smooth tire', *Applied Acoustics*, Vol. 26, No. 3, pp.181-192.

Kropp, W. (1999) 'A mathematical model of tyre noise generation', *International Journal of Heavy Vehicle Systems*, Vol. 6, No. 1-4, pp.310-329.

Kung, L.E. (1990) 'Radial vibration of pneumatic radial tires', *SAE Technical Paper 900759*.

Larsson, K. and Kropp, W. (2002) 'A high-frequency three-dimensional tire model based on two coupled elastic layers', *Journal of Sound and Vibration*, Vol. 253, No. 4, pp.889-908.

Lopez, I., Blom, R.E.A., Roozen, N.B. and Nijmeijer, H. (2007) 'Modelling vibrations on deformed rolling tyres - a modal approach', *Journal of Sound and Vibration*, Vol. 307, No. 3-5, pp.481-494.

Lopez, I., van Doorn, R.R.J.J., van der Steen, R., Roozen, N.B. and Nijmeijer, H. (2009) 'Frequency loci veering due to deformation in rotating tyres', *Journal of Sound and Vibration*, Vol. 324, No. 3-5, pp.622-639.

Mace, B.R., Duhamel, D., Brennan, M.J. and Hinke, L. (2005) 'Finite element prediction of wave motion in structural waveguides', *Journal of the Acoustical Society of America*, Vol. 117, No. 5, pp.2835-2843.

Mead, D.J. (1996) 'Wave propagation in continuous periodic structures: research contributions from Southampton', *Journal of Sound and Vibration*, Vol. 190, No. 3, pp.495-524.

Muggleton, J.M., Mace, B.R. and Brennan, M.J. (2003) 'Vibrational response prediction of a pneumatic tyre using an orthotropic two-plate wave model', *Journal of Sound and Vibration*, Vol. 264, No. 4, pp.929-950.

Narasimha Rao, K.V. and Kumar, R.K. (2007) 'Simulation of tire dynamic behavior using various finite element techniques', *International Journal for Computational Methods in Engineering Science and Mechanics*, Vol. 8, No. 5, pp.363-372.

Nguyen, H. (2008) *Une nouvelle approche pour structures périodiques; Application au calcul des vibrations d'un pneumatique*, PhD thesis, Ecole Nationale des Ponts et Chaussées, France.

Pacejka, H.B. (1971) 'The Tire as a Vehicle Component (Tire in-plane dynamics)', *Mechanics of pneumatic tires*, NBS Monograph 122, S.K. Clark, Ed., pp.741, (U.S. Government Printing Office, Washington, D.C.).

Padovan, J. (1976) 'On viscoelasticity and standing wave in tires', *Tire Science and Technology*, Vol. 4, No. 4, pp.233-246.

Périsse, J. and Hamet, J.F. (2000) 'A comparison of the 2d ring and 3d orthotropic plate for modelling of radial tire vibrations', *Inter-noise 2000*, Nice, France.

Périsse, J., Clairet, J.M. and Hamet, J.F. (2000) 'Modal testing of a smooth tire in low and medium frequency-estimation of structural parameters', *IMAC XVIII*, San Antonio, pp.960-967.

Périsse, J. (2002) 'A study of radial vibrations of a rolling tyre for tyre-road noise characterisation', *Mechanical systems and signal processing*, Vol. 16, No. 6, pp.1043-1058.

Pinnington, R.J., Briscoe, A.R. (2002) 'A wave model for a pneumatic tire belt', *Journal of Sound and Vibration*, Vol. 253, No. 5, pp.969-987.

Pinnington, R.J. (2006) 'A wave model of a circular tyre. Part 1: belt modelling', *Journal of Sound and Vibration*, Vol. 290, No. 1-2, pp.101-132.

Pinnington, R.J. (2006) 'A wave model of a circular tyre. Part 2: side-wall and force transmission modelling', *Journal of Sound and Vibration*, Vol. 290, No. 1-2, pp.133-168.

Potts, G.R., Bell, C.A., Charek, L.T. and Roy, T.K. (1977) 'Tire vibrations', *Tire Science and Technology*, Vol. 5, No. 4, pp.202-225.

Qatu, M.S., Abdelhamid, M.K., Pang, J. and Sheng, G. (2009) 'Overview of vehicle noise and vibration', *International Journal of Vehicle Noise and Vibration*, Vol. 5, No. 1-2, pp.1-35

Qatu, M.S. (2012) 'Recent research on vehicle noise and vibration', *International Journal of Vehicle Noise and Vibration*, Vol. 8, No. 4, pp.289-301

Richards, T.L. (1991) 'Finite element analysis of structural-acoustic coupling in tyres', *Journal of Sound and Vibration*, Vol. 149, No. 2, pp.235-243.

Tielking, J.T. (1965) 'Plane vibration characteristics of a pneumatic tire model', *SAE Paper 650492*.

Vu, T.D., Duhamel, D., Abbadi, Z., Yin, H.P. and Gaudin A. (2017) 'A nonlinear circular ring model with rotating effects for tire vibrations', *Journal of Sound and Vibration*, Vol. 388, pp.245-271.

Waki, Y., Mace, B.R. and Brennan, M.J. (2009) 'Free and forced vibrations of a tire using a wave/finite element approach', *Journal of Sound and Vibration*, Vol. 323, No. 3-5, pp.737-756.

Wei, Y.T., Nasdala, L. and Rothert, H. (2008) 'Analysis of forced transient response for rotating tires using REF models', *Journal of Sound and Vibration*, Vol. 320, No. 1-2, pp.145-162.

Zhang, X., Rakheja, S. and Ganesan, R. (2004) 'Modal analysis of a truck tyre using FE tyre model', *International Journal of Heavy Vehicle Systems*, Vol. 11, No. 2, pp.133-154.

Appendix A

In this section, the determination of the parameters required for the orthotropic plate model is described.

Foundation stiffness

The effect of sidewalls and the inflation pressure are represented by the foundation stiffness, s. For a freely suspended tire, the interaction between the tire and the rim can be considered as a simple mass-spring-mass system, in which the tire structure and the rim correspond to the masses and the foundation represents the spring stiffness. To this end, the mobility can be written as

$$Y(\omega) = \frac{i\omega(k - \omega^2 m_{rim})}{\omega^2[\omega^2 m_{rim} m_{tire} - k(m_{rim} + m_{tire})]}, \tag{22}$$

where k is the spring stiffness. When we consider the anti-resonance of the system, i.e. $k - \omega^2 m_{rim} = 0$, the foundation stiffness can be determined as

$$s = \frac{k}{l_x l_y} = \frac{\omega_1^2 m_{rim}}{l_x l_y}, \tag{23}$$

where ω_1 is the anti-resonance. The damping can be estimated by the half-power bandwidth around the anti-resonance.

Bending stiffness; tangential and lateral

As it is known, at higher frequencies, the behaviour of the tire structure is the same as a plate. The mobility of a plate is computed as

$$Y = \frac{1}{8\sqrt{m\sqrt{B_{xy}}}}. \tag{24}$$

Therefore, if we fit this equation to the data given by 3D models at high frequencies, the mixed bending stiffness, B_{xy} can be obtained. Assuming that $B_{xy} = B_x B_y$ and

$B_x = 2B_y$, one can determine B_x and B_y.

Tension

In order to calculate the tension, caused by the inflation pressure in the tire, it is supposed that the lateral direction vibrates only in the fundamental mode. When we substitute the resonance frequencies obtained from the frequency response of the 3D model, into Eq. 17, T_{x0} and T_{y0} can be estimated.